ARTICLES
https://doi.org/10.1038/s41593-018-0194-1
nature neuroscience

Pathogenic tau-induced piRNA depletion promotes neuronal death through transposable element dysregulation in neurodegenerative tauopathies

Wenyan Sun[1,2,3], Hanie Samimi[4], Maria Gamez[1,3], Habil Zare[3] and Bess Frost[1,3,5*]

Transposable elements, known colloquially as 'jumping genes', constitute approximately 45% of the human genome. Cells utilize epigenetic defenses to limit transposable element jumping, including formation of silencing heterochromatin and generation of piwi-interacting RNAs (piRNAs), small RNAs that facilitate clearance of transposable element transcripts. Here we utilize *Drosophila melanogaster* and postmortem human brain samples to identify transposable element dysregulation as a key mediator of neuronal death in tauopathies, a group of neurodegenerative disorders that are pathologically characterized by deposits of tau protein in the brain. Mechanistically, we find that heterochromatin decondensation and reduction of piwi and piRNAs drive transposable element dysregulation in tauopathy. We further report a significant increase in transcripts of the endogenous retrovirus class of transposable elements in human Alzheimer's disease and progressive supranuclear palsy, suggesting that transposable element dysregulation is conserved in human tauopathy. Taken together, our data identify heterochromatin decondensation, piwi and piRNA depletion and consequent transposable element dysregulation as a pharmacologically targetable, mechanistic driver of neurodegeneration in tauopathy.

Transposable elements are categorized as class I, the retrotransposons, or class II, the DNA transposons. Retrotransposons are structurally akin to retroviruses in that they require an RNA intermediate to mobilize. Unlike retroviruses, however, retro transposons lack the ability to move between individuals. DNA transposons, which mobilize via a 'cut and paste' mechanism, are thought to have lost the ability to mobilize in the human genome as a result of imprecise excision and insertion[1]. Organisms ranging from yeast to humans have developed cellular control mechanisms to limit potentially deleterious transposable element activation. Many transposable elements are embedded within highly condensed constitutive heterochromatin and are thus epigenetically silenced[2]. In addition, transposable element transcripts are the targets of a well-conserved pathway involving piRNAs, small regulatory RNAs that bind to transposable element transcripts and mediate their degradation[3].

The transposon theory of aging posits that transposable elements become deleteriously activated as cellular defense and surveillance mechanisms break down with age[4,5]. While transposable element activation has also been implicated in cancer[6] and in TDP-43-mediated neurodegeneration[7–9], the extent to which transposable elements are involved in human disorders and drive disease pathogenesis is unknown. We have previously identified tau-induced decondensation of constitutive heterochromatin as a key event that mediates neuronal death in tauopathy[10]. We hypothesized that tau-mediated decondensation of constitutive heterochromatin would cause epigenetic de-silencing of transposable elements in the context of Alzheimer's disease and associated tauopathies.

Beginning with a simple model of tauopathy in *Drosophila melanogaster*[11], we report significantly altered levels of transposable element transcripts as a consequence of human tau expression in the adult brain. We identify heterochromatin decondensation and depletion of piwi and piRNAs as mechanistic links between pathogenic tau and loss of transposable element control, and demonstrate that pathogenic tau causes active transposable element mobilization in neurons. Dietary restriction and lamivudine (3TC), a nucleoside analog inhibitor of reverse transcriptase that is FDA-approved for the treatment of HIV and hepatitis B, suppress tau-induced transposable element dysregulation and tau-induced neurotoxicity. Using a systematic, unbiased approach, we identify transposable elements that are differentially expressed in postmortem human brain tissue from patients with Alzheimer's disease and progressive supranuclear palsy, a primary tauopathy, and find that the endogenous retrovirus class of transposable elements is increased in the context of human tauopathy. Taken together, our studies identify heterochromatin decondensation and depletion of piwi and piRNAs as key mechanisms driving transposable element dysregulation and subsequent neuronal death in tau-mediated neurodegeneration. In addition, we show that that suppression of transposable element mobilization and resulting neurodegeneration can be achieved by environmental and pharmacological intervention.

Results

***Drosophila* models of human tauopathy have altered levels of transposable element transcripts.** *D. melanogaster* provides a genetically tractable platform that can be used to identify cellular mechanisms implicated in disease states and to determine whether they are causal for the disease process. To investigate a potential role for transposable element dysregulation as a consequence of pathogenic tau, we began with a *Drosophila* model of tauopathy[11]

[1]Barshop Institute for Longevity and Aging Studies, San Antonio, Texas, USA. [2]Department of Nutrition and Food Security, School of Public Health, Xi'an Jiaotong University, Xi'an, China. [3]Department of Cell Systems and Anatomy, University of Texas Health San Antonio, San Antonio, Texas, USA. [4]Department of Computer Science, Texas State University, San Marcos, Texas, USA. [5]Glenn Biggs Institute for Alzheimer's & Neurodegenerative Diseases, San Antonio, Texas, USA. *e-mail: bfrost@uthscsa.edu

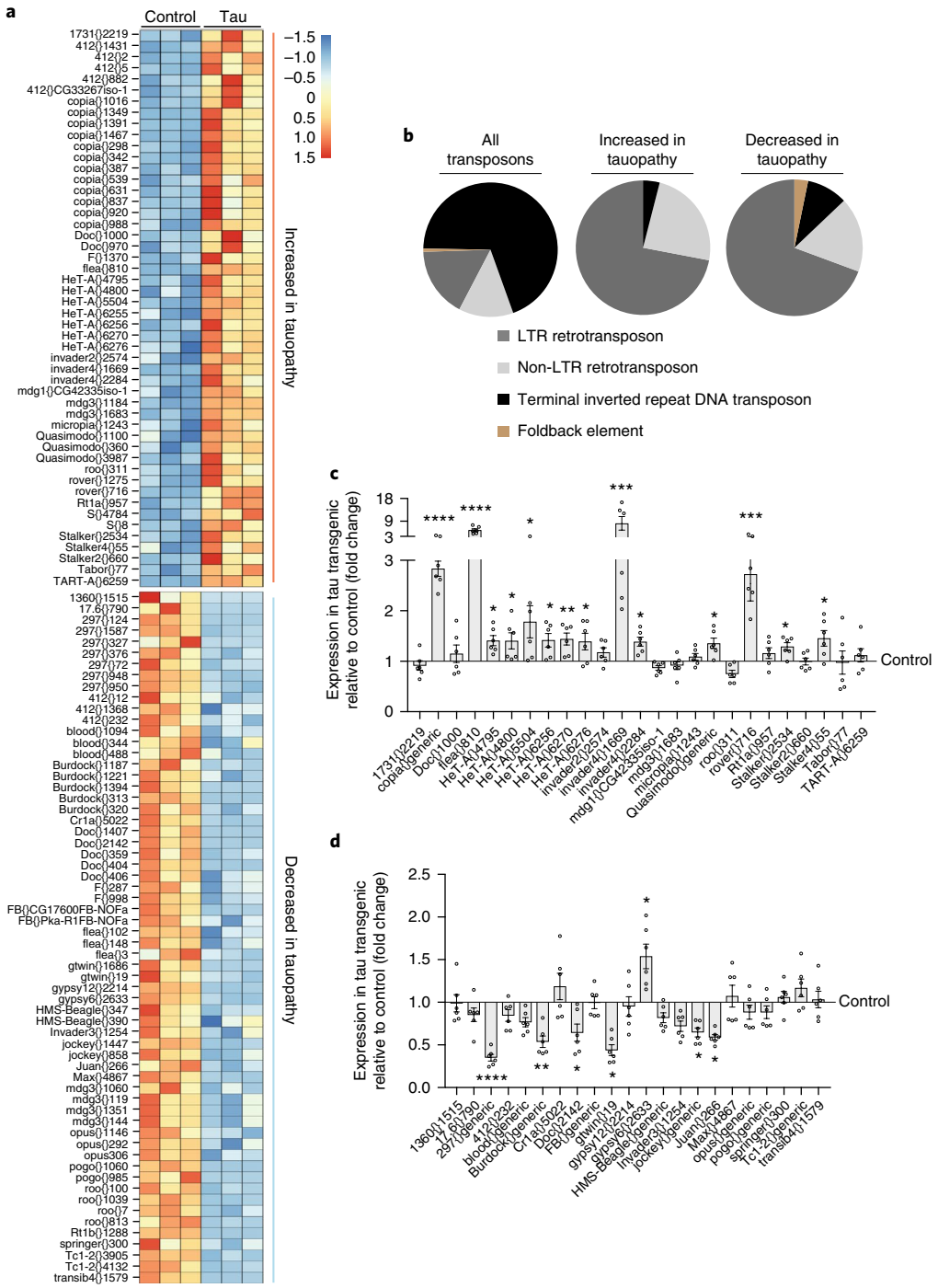

Fig. 1 | Transposable element transcription in tau^{R406W} transgenic *Drosophila*. a, Transposable element transcripts that are differentially expressed in tau^{R406W} transgenic *Drosophila* heads versus control by RNA-seq (two-sided Wald test, FDR, $P < 0.01$, $n = 3$ biologically independent replicates, each consisting of RNA pooled from 6 heads). **b**, Pie charts depicting all classes of transposable elements in *Drosophila*, and classes of transposable elements that are increased or decreased in tau^{R406W} transgenic *Drosophila*. **c**,**d**, NanoString-based validation of transposable element transcripts that are increased in tauopathy by RNA-seq (**c**) and transposable elements transcripts that are decreased in tau^{R406W} transgenic *Drosophila* by RNA-seq (**d**); $n = 6$ biologically independent replicates, each consisting of RNA pooled from 6 heads; values are relative to control, which was set to 1. Unpaired, two-tailed Student's *t*-test, $^{*}P < 0.05$, $^{**}P < 0.01$, $^{***}P < 0.001$, $^{****}P < 0.0001$. Values are mean ± s.e.m. All flies are 10 d old. Full genotypes are listed in Supplementary Table 1. Transposable elements recognized by generic probes are listed in Supplementary Table 4.

involving neuron-specific expression of tau^{R406W}, a mutant form of human tau that is associated with autosomal dominant tauopathy[12]. *Drosophila* models of human tauopathy have progressive, age-associated neuronal death, a shortened lifespan, and decreased locomotor activity[10,11]. In addition, neuronal phenotypes of tau transgenic *Drosophila* mimic features of human Alzheimer's disease and associated tauopathies, including but not limited to aberrant tau phosphorylation[13], oxidative stress[14], DNA damage[15,16],

decondensation of constitutive heterochromatin[10], synaptic dysfunction[17] and activation of the cell cycle in postmitotic neurons[18].

We performed 100-bp, paired-end sequencing of RNA isolated from control and tau^{R406W} transgenic *Drosophila* heads at day 10 of adulthood, an age at which neuronal death and locomotor deficits are detectable in tau^{R406W} transgenic flies but before the age at which survival is at exponential decline[16]. We identified 50 transposable elements that were significantly increased at the transcript level in tau transgenic *Drosophila* compared to controls and 60 transposable elements that were significantly decreased (Fig. 1a, Supplementary Fig. 1 and Supplementary Tables 1 and 2). For several subgroups of transposable elements, we found that multiple members of the same subgroup, such as *copia*, *HeT-A* and *Quasimodo*, were increased in tau^{R406W} transgenic *Drosophila* while members of other subgroups, such as *Burdock* and *Blood*, were decreased in tau^{R406W} transgenic *Drosophila*. These data suggest that aberrant expression of transposable elements in tauopathy is a regulated, rather than stochastic, process. The most abundant class of differentially expressed elements in tauopathy were class I long terminal repeat (LTR) retrotransposons, even though the majority of transposable elements in *Drosophila* are classified as class II DNA transposons (Fig. 1b).

The complexity and repetitive nature of transposable elements present challenges to RNA sequencing (RNA-seq) analysis, which is associated with a greater frequency of false positives and negatives compared to analysis of canonical messenger RNAs. As secondary validation of our RNA-seq analyses, we prepared a custom NanoString codeset consisting of a panel of probes recognizing transposable elements that were identified as differentially expressed in tau transgenic *Drosophila* by RNA-seq (Supplementary Table 3). NanoString technology combines transcript-specific color-coded barcodes with fluorescence imaging to sensitively quantify transcript levels[19]. When possible, we created 'generic' NanoString probes to recognize the differentially expressed transposable elements within a transposable element subgroup (Supplementary Table 4). While a calculation of the fold-change estimate for each element generated by RNA-seq versus the fold-change for NanoString (Supplementary Fig. 1b) suggests a moderate to strong relationship between RNA-seq and NanoString, not all transposable elements that were called as differentially expressed in tau transgenic *Drosophila* by RNA-seq reached statistical significance by NanoString analysis. Fourteen of 25 probes were confirmed by NanoString as significantly increased in heads of tau^{R406W} transgenic *Drosophila* (Fig. 1c), while 6 of 22 probes were confirmed as significantly decreased (Fig. 1d). These analyses also revealed that the transposable elements transcripts that increased in response to pathogenic tau generally had a greater magnitude of change than transposable element transcripts that decreased in response to pathogenic tau.

We hypothesized that aberrant transposable element expression would be relevant to the larger group of tauopathies, including Alzheimer's disease, that are pathologically defined by deposition of wild-type tau in the brain. To test this hypothesis, we assayed transposable element transcript levels by NanoString in *Drosophila* expressing human wild-type tau (tau^{WT}; Supplementary Fig. 2a), which induces neuronal death in *Drosophila*[11], albeit to a lesser extent than tau^{R406W}. Multiple previous studies report that expression of human wild-type and R406W mutant tau involves the same main mechanisms of tau-induced neurotoxicity in *Drosophila* models[10,16,20]. Pan-neuronal expression of tau^{WT} significantly increased 10 of 25 and decreased 8 of 22 probes recognizing transposable elements that were identified as increased or decreased, respectively, in tau^{R406W} *Drosophila* by RNA-seq (Supplementary Fig. 2b,c), suggesting that aberrant transposable element expression is relevant to the greater family of sporadic tauopathies that involve only wild-type tau.

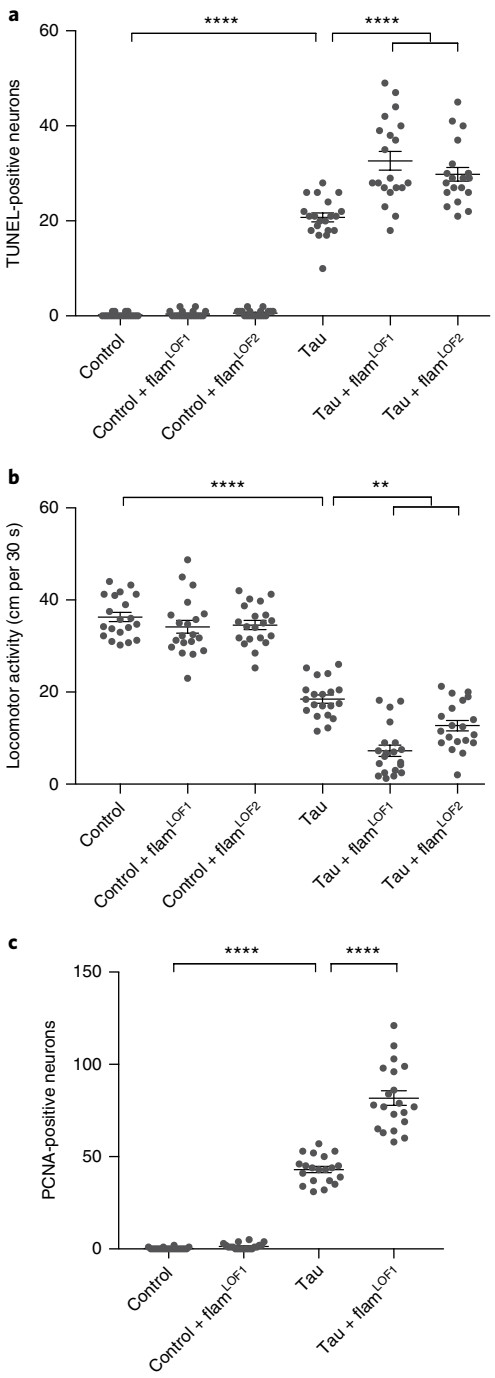

Fig. 2 | Loss-of-function mutations in the *flamenco* locus enhance tau^{R406W}-induced neurotoxicity. (**a**–**c**) Compared to tau^{R406W} expressed alone, tau^{R406W} transgenic *Drosophila* harboring loss-of-function mutations in the *flamenco* locus have increased neuronal death as assessed by TUNEL (**a**; one-way ANOVA with Tukey's multiple comparison test), reduced locomotor activity (**b**; one-way ANOVA with Tukey's multiple comparison test) and increased activation of the cell cycle as assessed by PCNA staining (**c**; one-way ANOVA with Tukey's multiple comparison test). $n = 20$ animals per genotype per assay. All flies were 10 d old. Values are mean ± s.e.m. $n = 20$ animals per genotype per assay, $^{**}P = 0.005$, $^{***}P < 0.001$, $^{****}P < 0.0001$. Full genotypes are listed in Supplementary Table 1.

Loss of transposable element silencing mediates tau-induced neurotoxicity in *Drosophila*. RNA-seq and NanoString analyses clearly demonstrated that pathogenic tau disrupts baseline levels of

transposable element transcripts in the brain. Transposable element activation is classically considered a deleterious event, as mobilization can cause genomic instability[21]. It is now understood, however, that transposable element RNAs have regulatory roles within the cell[1]. In addition, active transposable element mobilization during neurogenesis is thought to positively contribute to somatic diversification[22]. To establish whether dysregulation of transposable element expression in the adult brain is beneficial, detrimental or neutral in the context of tauopathy, we tested whether genetic manipulation of *flamenco*, a locus in *Drosophila* that is known to restrict transposable element mobilization, would modify tau^{R406W}-induced neurotoxicity. Homozygous 'permissive' loss-of-function alleles of *flamenco* allow transposable element mobilization and increase transposable element copy number within the *Drosophila* genome[23,24]. Two different heterozygous loss-of-function alleles of *flamenco*[23,24] did not induce neuronal death or locomotor deficits in controls, but significantly enhanced neuronal death in tau^{R406W} transgenic *Drosophila* (Fig. 2a) and exacerbated tau-induced locomotor deficits (Fig. 2b). Importantly, *flamenco* mutations did not affect total protein levels of transgenic tau (Supplementary Fig. 3a).

Ectopic expression of proteins associated with aberrant activation of the cell cycle in postmitotic neurons is a well-described feature of human tauopathy[25]. Studies in *Drosophila* indicate that cell cycle activation causes neuronal death in tauopathy and that activation of the cell cycle in neurons is sufficient to induce neuronal death[18]. We found that heterozygous loss of *flamenco* function exacerbated tau-induced activation of the cell cycle in neurons as assessed by staining with an antibody recognizing proliferating cell nuclear antigen (PCNA) (Fig. 2c). Taken together, these data suggest that loss of transposable element silencing in tau transgenic *Drosophila* is causally linked to neuronal death and promotes neuronal death through aberrant activation of the cell cycle in postmitotic neurons.

The *flamenco* locus harbors piRNAs that specifically degrade *gypsy*, *Idefix* and *ZAM* transposable element transcripts[24], among others. To determine whether *flamenco* mutation affects the specific panel of transposable elements that are aberrantly expressed in tau^{R406W} transgenic *Drosophila*, we performed NanoString analyses on *flamenco* loss-of-function mutants (Supplementary Fig. 3). Rather than a general effect on the panel of transposable elements that are dysregulated by pathogenic tau, these analyses suggested that enhancement of tau-induced neurotoxicity by *flamenco* loss of function was due to activation of specific elements affected by pathogenic tau and/or additional elements outside of our NanoString codeset.

Piwi and piRNA depletion is a mechanistic driver of transposable element transcription in tauopathy. Since *flamenco* is known to encode a major piRNA cluster[3,26] and piRNAs have recently been reported to be differentially expressed in the brain in human Alzheimer's disease[27,28], we next determined whether piRNAs are involved in dysfunctional transposable element control in the tauopathy-affected *Drosophila* brain. Small RNA sequencing revealed a significant decrease in 46 of 50 differentially expressed piRNAs in heads of tau transgenic *Drosophila* at day 10 of adulthood (Fig. 3a and Supplementary Tables 5 and 6). In addition, protein levels of piwi, a central regulator of piRNA biogenesis, were depleted in brains of tau transgenic *Drosophila* as assessed by both immunofluorescence (Fig. 3b) and western blotting (Fig. 3c).

While the function of piwi in regard to piRNA production and transposable element silencing is well established in the germline[29], and piRNAs are known to exist in the *Drosophila* and mammalian brain[30,31], it is unknown whether piwi reduction affects transposable element transcripts in the brain. To directly quantify the effects of piwi reduction on the panel of transposable elements that were differentially expressed in tau^{R406W} transgenic *Drosophila*, we used our custom NanoString codeset to assay transposable element transcript levels in response to pan-neuronal RNA interference (RNAi)-mediated piwi knockdown in the absence of transgenic tau. These data indicated that pan-neuronal piwi knockdown (Supplementary Fig. 4a) was sufficient to elevate transcript levels of most of the transposable elements that are increased in tau^{R406W} transgenic *Drosophila* (Fig. 3d), suggesting that tau-induced reduction of piwi and piRNAs is a major contributor to the transposable element expression profile in brains of tau transgenic *Drosophila*.

We next determined whether piwi depletion is a causal mediator of neuronal death in tauopathy. RNAi-mediated piwi knockdown using two different, non-overlapping RNAi lines was semi-lethal in the context of transgenic tau expression. In the absence of tau, piwi knockdown was sufficient to induce neuronal death by day 10 of adulthood (Fig. 3e). Per PCNA staining, pan-neuronal piwi reduction was also sufficient to activate the cell cycle in neurons (Supplementary Fig. 4b), suggesting that pathogenic tau acts through piwi reduction to mediate aberrant cell cycle activation and consequent neuronal death.

We next determined whether pan-neuronal overexpression of piwi[32] would reduce aberrant transposable element expression and neuronal death in brains of tau transgenic *Drosophila*. Compared to tau expressed alone, piwi overexpression significantly reduced transposable element transcripts that are elevated in tau transgenic *Drosophila* (Fig. 3f). In further support of piwi reduction as a causal contributor to tau-induced neurotoxicity, pan-neuronal piwi overexpression significantly reduced neuronal death in tau transgenic *Drosophila* (Fig. 3g) without affecting total levels of transgenic tau protein (Supplementary Fig. 4c). These data suggest that tau-induced piwi reduction depletes piRNAs, which significantly increases transposable element transcripts and causally contributes to tau-induced neurotoxicity.

Fig. 3 | Decreased expression of piwi and piRNAs mediate pathogenic tau^{R406W}-induced increase in transposable element transcripts and drive neuronal death. a, Heat map reflecting fold change of piRNAs that are differentially expressed in tau^{R406W} transgenic *Drosophila* heads versus controls as assessed by small RNA-seq (two-sided Wald test, FDR, $P < 0.01$, $n = 4$ biologically independent replicates, each consisting of RNA pooled from 6 heads). **b**,**c**, Decreased levels of piwi protein (red) in cortex of the tau^{R406W} transgenic *Drosophila* brain as assessed by immunostaining (b) and western blotting (c) (unpaired, two-tailed Student's *t*-test, $^{**}P = 0.005$, $n = 6$ animals per genotype). In b, piwi immunostaining was repeated in 6 animals of each genotype with similar results. Western blot is cropped in c; full blot presented in Supplementary Fig. 10. **d**, NanoString analysis of transposable element expression in response to RNAi-mediated knockdown of piwi versus control (unpaired, two-tailed Student's *t*-test, $^{*}P < 0.05$, $^{**}P < 0.01$, $^{***}P < 0.001$, $^{****}P < 0.0001$; $n = 6$ biologically independent replicates, each consisting of RNA pooled from 6 heads; values are relative to control, which was set to 1). **e**, Neuronal death assayed by TUNEL in *Drosophila* caused by pan-neuronal RNAi-mediated knockdown of *piwi* (one-way ANOVA with Tukey's multiple comparison test, $^{****}P < 0.0001$, $n = 20$ animals per genotype). **f**, NanoString analysis of transposable element expression in response to pan-neuronal piwi overexpression in tau^{R406W} transgenic *Drosophila* versus tau expressed alone (unpaired, two-tailed Student's *t*-test, $^{*}P < 0.05$, $^{**}P < 0.01$, $^{***}P < 0.001$, $^{****}P < 0.0001$; $n = 6$ biologically independent replicates, each consisting of RNA pooled from 6 heads; values are relative to tau expressed alone, which was set to 1). **g**, Neuronal death assayed by TUNEL in tau^{R406W} transgenic *Drosophila* with pan-neuronal piwi overexpression (one-way ANOVA with Tukey's multiple comparison test, $^{****}P < 0.0001$, $n = 20$ animals per genotype). All flies were 10 d old. Values are mean ± s.e.m. Full genotypes are listed in Supplementary Table 1. Transposable elements recognized by generic probes are listed in Supplementary Table 4.

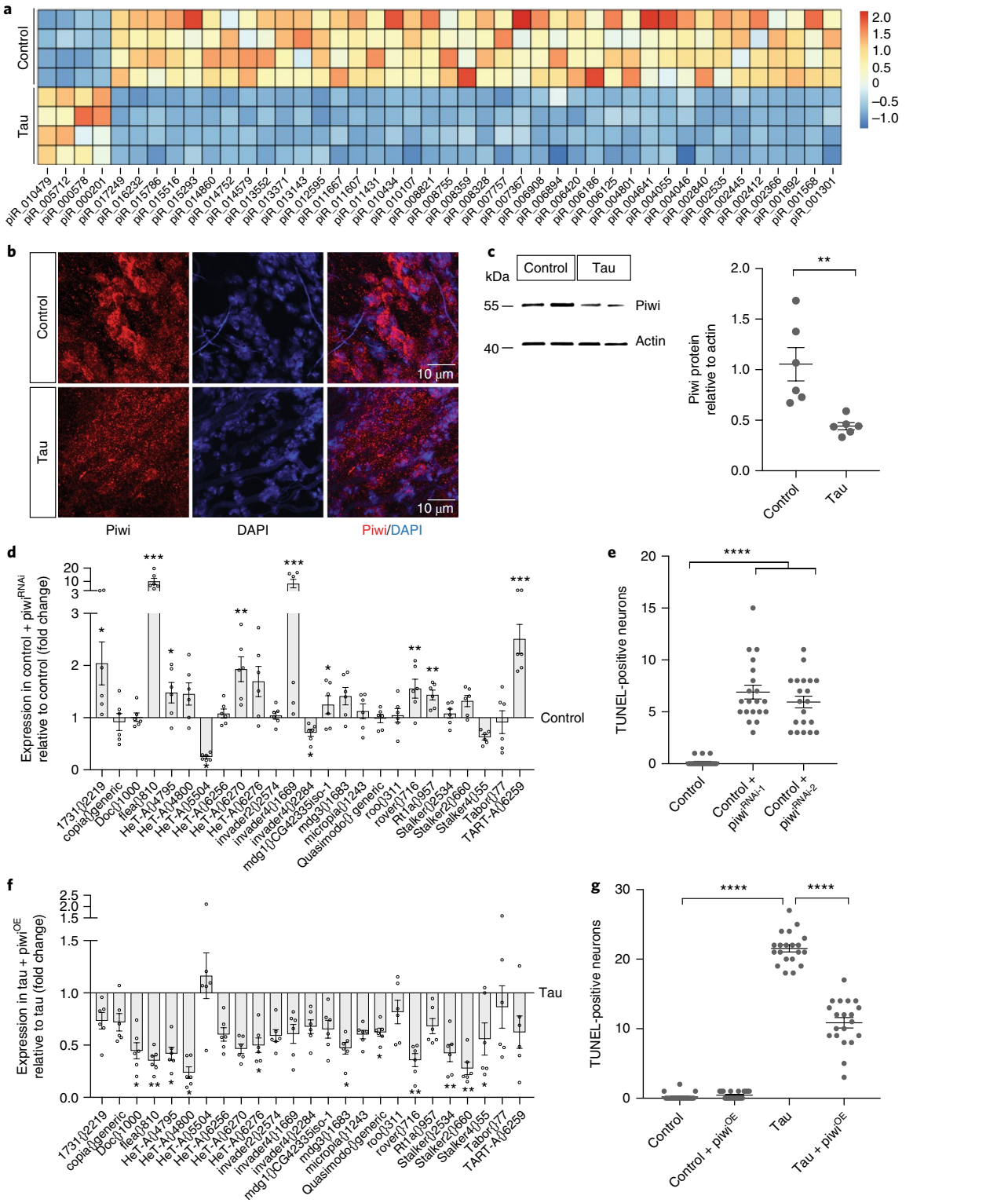

Decondensation of heterochromatin contributes to aberrant transposable element transcription in the adult *Drosophila* brain. We have previously reported widespread relaxation of constitutive heterochromatin, a form of hypercondensed DNA, in post-mortem brains from patients with Alzheimer's disease, which is the most common tauopathy, and in *Drosophila* and mouse models of tauopathy[10]. Tau-induced heterochromatin relaxation mediates neurodegeneration, as loss-of-function mutations in *Su(var)205*[33] and *Su(var)3-9*[34], genes, encoding heterochromatin protein 1 (HP1) and a histone 3 Lys9 methyltransferase, respectively, further deplete constitutive heterochromatin in tau transgenic *Drosophila* and enhance tau-induced neuronal death[10].

On the basis of previous studies that identified constitutive heterochromatin as a silencing mechanism for transposable elements[35], we next determined whether genetically promoting heterochromatin relaxation would affect the transposable elements that are differentially expressed in tau transgenic *Drosophila*. NanoString analyses showed that genetically promoting heterochromatin relax-

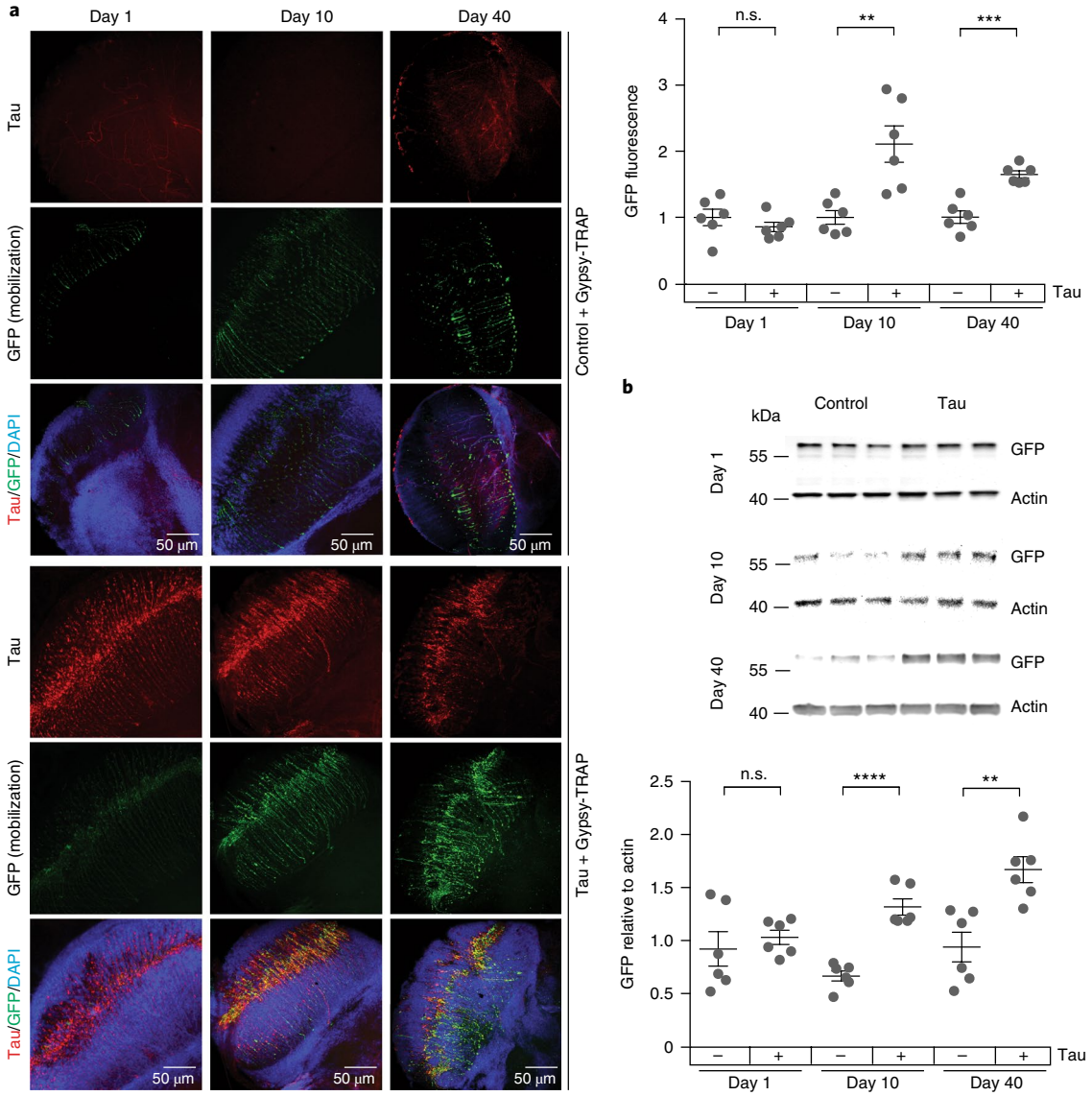

Fig. 4 | Active mobilization of transposable elements in neurons of tau transgenic *Drosophila*. a, Gypsy-TRAP (GFP, green), a reporter of transposable element mobilization, is activated in retinal neurons of 10- and 40-d-old tau^{V337M} transgenic *Drosophila* compared to control. Brains were stained with the cTau antibody (red) to recognize transgenic tau (unpaired, two-tailed Student's *t*-test, $n=6$ animals per genotype per age; n.s., not significant; $^{**}P=0.004$, $^{***}P=0.0001$). **b**, Quantification of gypsy-TRAP activation by western blotting with an antibody recognizing GFP (unpaired, two-tailed Student's *t*-test; n.s., not significant; $^{**}P=0.003$, $^{****}P<0.0001$). Western blot is cropped; full blot presented in Supplementary Fig. 10. $n=6$ animals per genotype per age. Values are mean ± s.e.m. Full genotypes are listed in Supplementary Table 1.

ation by loss-of-function mutations in *Su(var)205* or *Su(var)3-9* caused an increase in most of the transposable element transcripts that were identified as significantly increased in tau transgenic *Drosophila* by RNA-seq (Supplementary Fig. 5a,b). In the context of our previous report identifying tau-induced heterochromatin decondensation as a central mediator of neurotoxicity in tauopathy, these data suggest that tau-induced heterochromatin decondensation contributes to transposable element dysregulation in brains of tau transgenic *Drosophila*.

Active transposable element mobilization in neurons of tau transgenic *Drosophila*. Fifty-six percent of the transposable element transcripts that were significantly increased in tau transgenic *Drosophila* were full-length class I retrotransposons that are fully capable of mobilization. As transcription of DNA to RNA is the first step in retrotransposon mobilization, we next determined whether transposable elements actively mobilize in the context of tauopathy. Specifically, we used the gypsy-TRAP reporter, a GFP-based reporter of *copia* and/or *gypsy* insertion into the *ovo* locus that was developed to detect transposable element mobilization[4]. Because the gypsy-TRAP reporter utilizes the GAL4-*UAS* system that we normally use to express transgenic tau pan-neuronally, we instead used an existing tauopathy model that relies on direct fusion of the human tau transgene to *GMR*, a retinal neuron driver. These flies harbor the V337M disease-associated[12] form of human mutant tau.

Neuronal death in *Drosophila* models of tauopathy is age-dependent. Accordingly, we did not detect transposable element mobilization in tau^{V337M} transgenic *Drosophila* by either gypsy-TRAP GFP reporter fluorescence or immunoblotting at day 1 of adulthood, but detected a significant increase of transposable element mobilization in tau transgenic *Drosophila* by both GFP fluorescence and immunoblotting at day 10 of adulthood. The significant increase in transposable element mobilization in tauopathy compared to controls was sustained in 40-d-old adults (Fig. 4a,b).

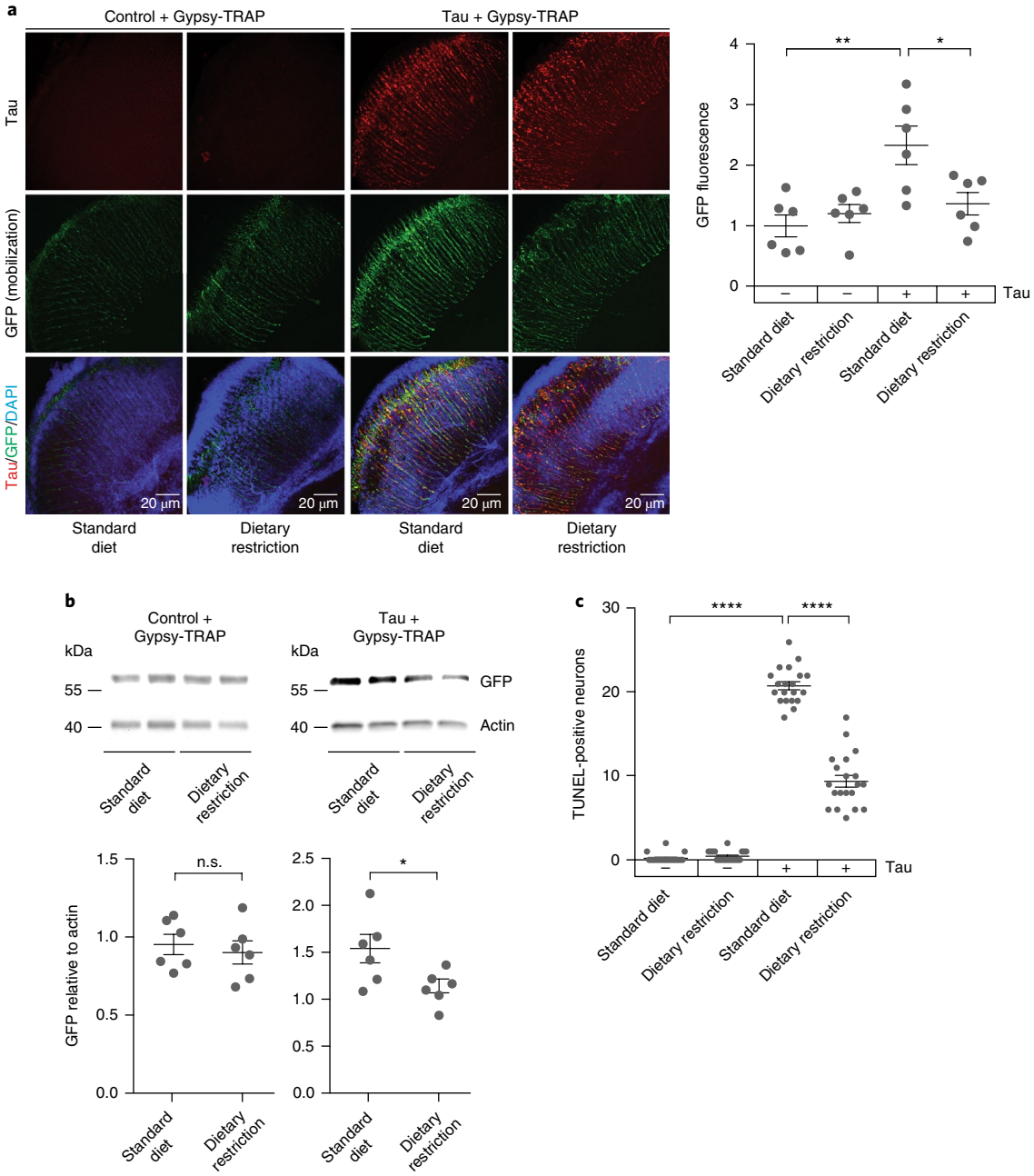

Fig. 5 | Dietary restriction significantly suppresses tau-induced transposable element mobilization and tau-induced neurotoxicity in *Drosophila*. **a**,**b**, Dietary restriction (66%) reduces gypsy-TRAP reporter activation in retinal neurons of tau^{V337M} transgenic *Drosophila* as assessed by GFP fluorescence (a; one-way ANOVA with Tukey's multiple comparison test, $^{*}P=0.03$, $^{**}P=0.002$, $n=6$ animals per genotype per treatment) and western blotting (b; unpaired, two-tailed Student's *t*-test; n.s., not significant; $^{*}P=0.04$, $n=6$ animals per genotype per treatment). Western blot is cropped in b; full blot presented in Supplementary Fig. 10. **c**, Dietary restriction (66%) significantly reduces tau^{R406W}-induced neuronal death assessed by TUNEL (one-way ANOVA with Tukey's multiple comparison test, $^{****}P<0.0001$, $n=20$ animals per genotype per treatment). All flies were 10 d old. Values are mean ± s.e.m. Full genotypes are listed in Supplementary Table 1.

Dietary restriction and inhibition of reverse transcriptase protect against tau-induced transposable element dysregulation and suppress neurotoxicity in tau transgenic *Drosophila*. Dietary restriction extends lifespan in invertebrate and vertebrate systems[36] and reduces age-related transposable element mobilization events in the *Drosophila* fat body[5]. Using the gypsy-TRAP GFP-based reporter of transposable element mobilization[4], we found that 66% dietary restriction reduced tau-induced transposable element mobilization in adult *Drosophila* neurons (Fig. 5a,b). As assessed by NanoString, dietary restriction significantly reduced the *copia* family at the transcript level, as well as several other transposable elements that were significantly increased in tau transgenic *Drosophila* (Supplementary Fig. 6). TUNEL revealed that dietary restriction suppressed tau-induced neuronal death (Fig. 5c).

Having established that tau-induced transposable element dysregulation is amenable to suppression, we took a pharmacological approach to reduce transposable element mobilization in tauopathy. Like retroviruses, retrotransposons encode machinery, including a capsid protein, polymerase, integrase and reverse transcriptase, needed to copy themselves and insert the new copy into

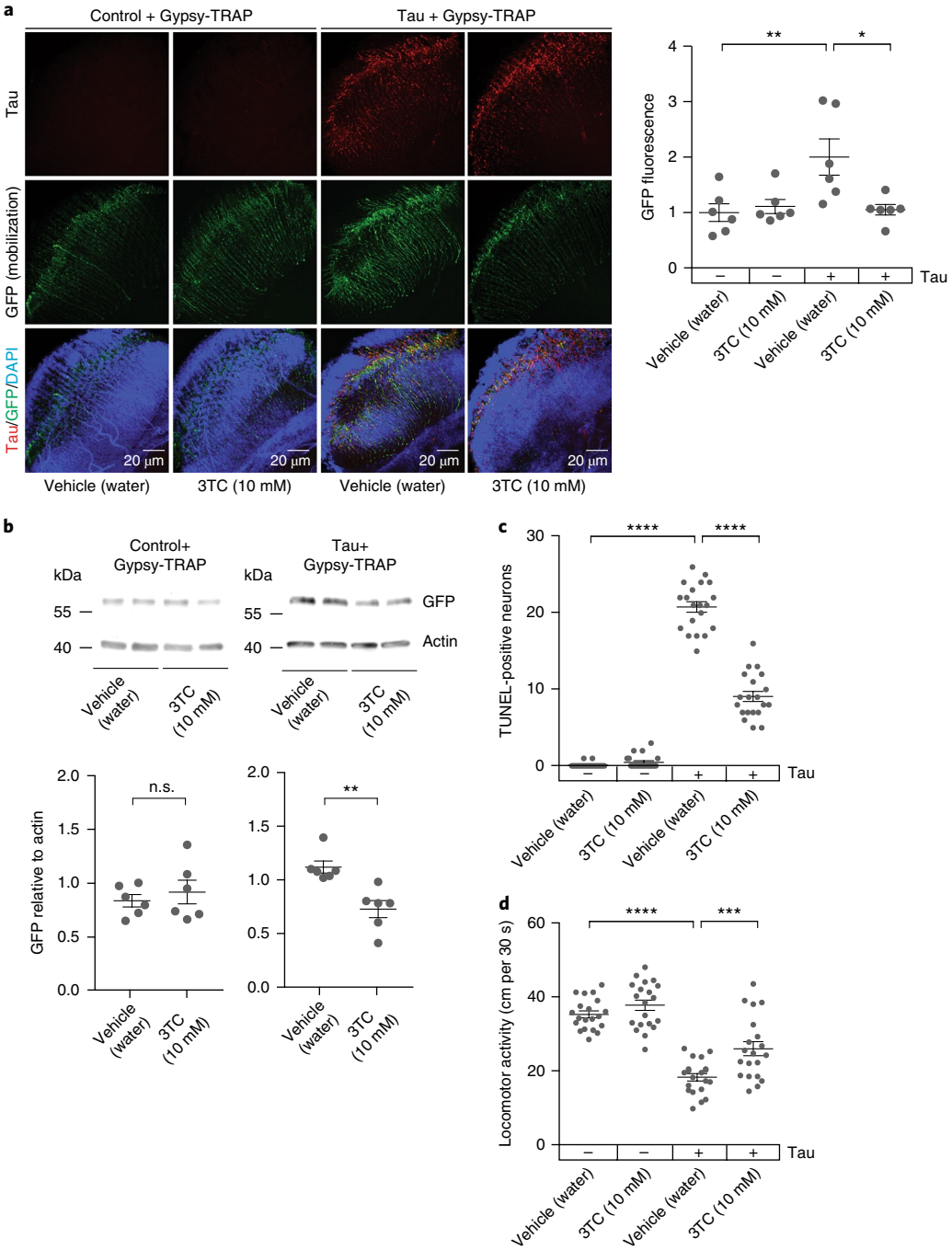

Fig. 6 | 3TC, an FDA-approved nucleoside analog reverse transcriptase inhibitor, suppresses tau-induced transposable element mobilization and tau-induced neurotoxicity in *Drosophila*. **a**,**b**, 10 mM 3TC reduces gypsy-TRAP reporter activation in retinal neurons of tau^{V337M} transgenic *Drosophila* as assessed by GFP fluorescence (**a**; one-way ANOVA with Tukey's multiple comparison test, $^{*}P = 0.01$, $^{**}P < 0.01$, $n = 6$ animals per genotype, per treatment) and western blotting (**b**; unpaired, two-tailed Student's *t*-test; n.s., not significant; $^{**}P = 0.003$, $n = 6$ animals per genotype per drug treatment). Western blot is cropped in b; full blot presented in Supplementary Fig. 10. **c**, 3TC (10 mM) significantly reduces tau^{R406W}-induced neuronal death assessed by TUNEL (one-way ANOVA with Tukey's multiple comparison test, $^{****}P < 0.0001$, $n = 20$ animals per genotype, per treatment). **d**, 3TC (10 mM) significantly alleviates tau^{R406W}-induced deficits in locomotor activity (one-way ANOVA with Tukey's multiple comparison test, $^{***}P = 0.0008$, $^{****}P < 0.0001$, $n = 20$ animals per genotype per treatment). All flies were 10 d old. Values are mean ± s.e.m. Full genotypes are listed in Supplementary Table 1.

the genome[37]. 3TC is a water-soluble nucleoside analog inhibitor of reverse transcriptase[38] that is FDA-approved for treatment of HIV and AIDS and of hepatitis B, both of which are caused by retroviruses. Like dietary restriction, 3TC is reported to reduce age-associated transposable element mobilization in the *Drosophila* fat body[5]. Tau transgenic flies treated with 10 mM 3TC had significantly reduced gypsy-TRAP reporter activation in the brain (Fig. 6a,b). In addition, 3TC treatment significantly reduced tau-induced neuronal death (Fig. 6c) and significantly alleviated tau-induced locomotor deficits (Fig. 6d) in a dose-dependent manner (Supplementary Fig. 7a,b). Taken together, these data provide further evidence that transposable element dysregulation causes the disease process in tauopathy and is responsive to environmental and pharmacological inhibition.

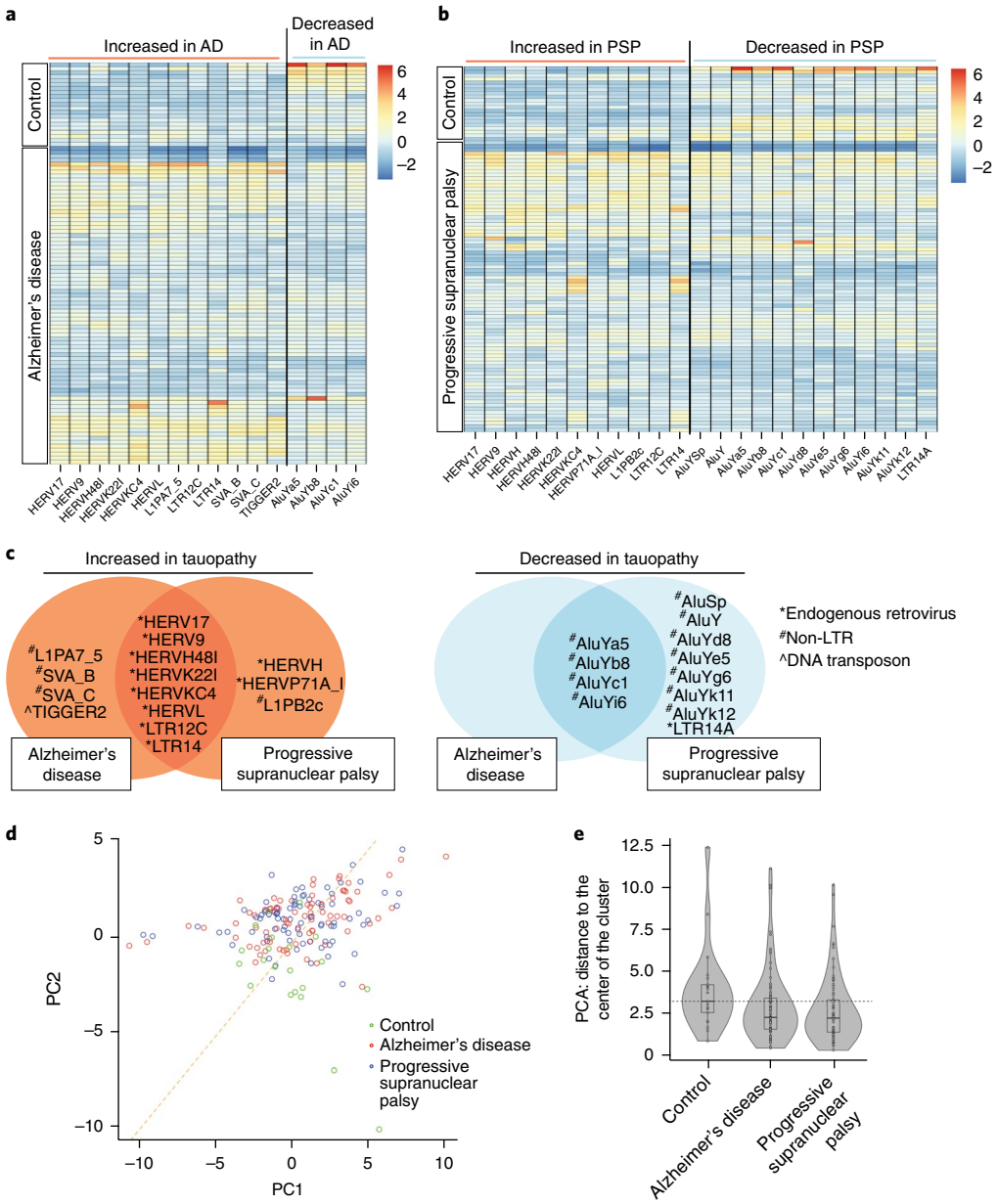

Fig. 7 | Transposable element expression in cortex of human tauopathy. a,**b**, Heat maps reflecting fold change of differentially expressed transposable elements in human cortex in control versus Alzheimer's disease (AD; **a**) and control versus progressive supranuclear palsy (PSP; **b**), as assessed by RNA-seq (two-sided Wald test, FDR, $P < 0.01$). **c**, Differentially expressed transposable elements in postmortem Alzheimer's disease and progressive supranuclear palsy cortex compared to controls. HERVs are significantly over-represented among transposable element transcripts that are increased in tauopathy (hypergeometric test, adjusted $P = 0.004$). Non-LTR elements are significantly over-represented among transposable elements that are decreased in tauopathy (hypergeometric test, adjusted $P = 4 \times 10^{-8}$). **d**, Principal component analyses of differentially expressed transposable elements in control, Alzheimer's disease and progressive supranuclear palsy cortex (two-sided Kolmogorov–Smirnov test, $P < 10^{-13}$). **e**, Based on principal component analysis of transposable element expression in control versus tauopathy, violin plots show that control samples are farther from the center of the cluster, as defined by the median of Alzheimer's disease and progressive supranuclear palsy samples. Euclidian distance was computed using the first two principal components (PCs) of those transposable elements that were differentially expressed among the three conditions. For control, AD and PSP respectively, minima = 0.8, 0.4, 0.3, maxima = 12.3, 11.1, 10.1, median = 3.2, 2.2, 2.2, mean = 3.8, 2.8, 2.6, first quartile = 2.5, 1.5, 1.3, third quartile = 4.2, 3.4, 3.2. In the violin plots, the center line corresponds to the median and the lower and upper hinges correspond to the first and third quartiles. The upper whisker extends from the upper hinge to the highest value within 1.5 IQR of the upper quartile, where IQR is the interquartile range (i.e., the distance between the first and third quartiles). The lower whisker extends to the smallest value. The outlier values beyond the end of the whiskers are plotted individually. Human control $n = 21$, Alzheimer's disease $n = 80$, progressive supranuclear palsy $n = 82$ biologically independent replicates in **a**–**e.**

Aberrant transposable element transcription in human tauopathy. We next analyzed transposable element expression in human tauopathy using RNA-seq data from cortex (Fig. 7a,b) and cerebellum (Supplementary Fig. 8a,b) of postmortem human controls and subjects with Alzheimer's disease and progressive supranuclear palsy (Supplementary Table 7). As in tau transgenic *Drosophila*, we found that specific subgroups of transposable elements were upregulated in human tauopathy while other subgroups were downregulated.

Among transposable elements that were upregulated in cortex and cerebellum of both tauopathies, we found a significant over-representation of endogenous retroviruses, while non-LTR retrotransposons were significantly over-represented among transposable elements that were downregulated in cortex and cerebellum of both tauopathies (Fig. 7c and Supplementary Fig. 8c).

We hypothesized that transposable element expression profiles of Alzheimer's disease and progressive supranuclear palsy would more closely resemble each other than controls. Principal component analysis supported this hypothesis; in particular, control samples had significantly lower values in the second principal component compared to Alzheimer's disease and progressive supranuclear palsy samples in both cortex (Fig. 7d) and cerebellum (Supplementary Fig. 8d). We computed the median of the first two principal components over all tauopathy samples and found that the distance of control samples to the median center was significantly further than in tauopathy samples in both cortex (Fig. 7e) and cerebellum (Supplementary Fig. 8e). Taken together, analyses of human transposable elements revealed a significant transcriptional increase in endogenous retroviruses and a significant decrease in non-LTR retroelements in postmortem human brain in both Alzheimer's disease and progressive supranuclear palsy. In addition, these data suggest that transposable element dysregulation in human tauopathy is a regulated rather than stochastic process, consistent with our studies in tau transgenic *Drosophila*.

Discussion

We have uncovered a therapeutically targetable mechanism whereby pathogenic tau drives neuronal death (Supplementary Fig. 9). Specifically, our studies identified dysregulation of transposable elements as a consequence of pathogenic tau and a driver of aberrant cell cycle activation in neurons and subsequent neuronal death. We identified genetic, dietary and pharmacological approaches to reduce transposable element dysregulation and suppress tau-induced neurotoxicity in *Drosophila*. We applied an unbiased transcriptomic approach to extend our findings to postmortem human brains and identified differentially expressed transposable elements in Alzheimer's disease and progressive supranuclear palsy.

Because the complexity and repetitive nature of transposable elements present challenges to RNA-seq analysis, which is associated with a greater frequency of false positives and negatives compared to analysis of canonical messenger RNAs, we performed secondary validation of differentially expressed transposable element transcripts in tau transgenic *Drosophila* by NanoString. While NanoString data showed a similar expression trend for most of the transposable elements that were identified as differentially expressed in tau transgenic *Drosophila* by RNA-seq, some of the elements were not confirmed as differentially expressed by NanoString. These data reveal the limitations of each assay when analyzing transposable element transcripts and stress the importance of rigorous secondary validation. Since many members of the *copia* family are increased at the transcript level in both RNA-seq and NanoString analyses, we speculate that gypsy-TRAP reporter activation is a result of *copia* insertion into the *ovo* locus, rather than *gypsy*. Our attempts to sequence de novo *copia* insertions within the *ovo* locus in homogenates prepared from tau transgenic *Drosophila* heads resulted in a high frequency of mismatches (data not shown), which is likely a result of the stochastic nature of transposable element insertion.

According to current understanding, cells have two layers of defense against potentially deleterious transposable element activation: transposable element transcription is limited by heterochromatin-mediated silencing, and transposable element transcripts are cleared from the cell by piRNA-mediated degradation. We found that both mechanisms of transposable element suppression were compromised in tauopathy. We speculate that tau-induced heterochromatin decondensation facilitates active transcription of transposable elements and that tau-induced piwi and piRNA reduction allows those transcripts to persist. While our results are consistent with the effects of heterochromatin decondensation and piwi reduction on transposable element expression that have been reported in the *Drosophila* germline[3,39], our studies reveal a previously undocumented role for heterochromatin- and piRNA-mediated transposable element silencing in the brain. On the basis of studies in the germline reporting a direct interaction between piwi and HP1[40] and a requirement for Rhino, a member of the HP1 subfamily, for piRNA production[41], it is possible that a direct interaction between piwi and HP1 is also required to silence transposable elements in the brain.

Among upregulated transposable elements in human tauopathy, the human endogenous retrovirus (HERV) family, including HERV-K, was significantly over-represented. Elevated HERV-K transcripts are associated with amyotrophic lateral sclerosis (ALS)[8] and many human cancers, including melanoma, breast cancer, germ cell tumors, renal cancer and ovarian cancer[42]. A causal association between HERV-K and neuronal dysfunction has previously been established, as ectopic expression of HERV-K or the retroviral envelope protein that it encodes decreases synaptic activity and induces progressive motor dysfunction in mice[8]. Antiretroviral reverse transcriptase inhibitors inhibit HERV-K activation in cultured cells[43] and are now in clinical trials for the treatment of ALS. On the basis of the data presented here, reverse transcriptase inhibitors have significant potential as a therapeutic strategy for the treatment of neurodegenerative tauopathies, including Alzheimer's disease.

The ability of *flamenco* loss-of-function mutations to enhance tau-induced neurotoxicity and the ability of piwi overexpression, dietary restriction and inhibition of reverse transcriptase to reduce transposable element dysregulation and suppress tau-induced neurotoxicity suggest that tau-induced transposable element dysregulation is deleterious to neuronal survival. In addition to the detrimental effects of transposable element jumping, double-stranded RNAs produced by transposable element transcripts, including HERVs, can trigger a type I interferon response through the innate immune system[44]. In light of the HERV increase in human tauopathy and the involvement of the innate immune response as a disease-promoting mechanism in Alzheimer's disease[45], it is tempting to speculate that expression of endogenous retroviruses in human tauopathy contributes to neuroinflammation, in addition to promoting genomic instability. In future studies, it will be important to investigate a potential effect of transposable element activation on the innate immune response in the context of tauopathy.

Methods

Methods, including statements of data availability and any associated accession codes and references, are available at https://doi.org/10.1038/s41593-018-0194-1.

Received: 17 November 2017; Accepted: 12 June 2018;
Published online: 23 July 2018

References

1. Chuong, E. B., Elde, N. C. & Feschotte, C. Regulatory activities of transposable elements: from conflicts to benefits. *Nat. Rev. Genet.* **18**, 71–86 (2017).
2. Slotkin, R. K. & Martienssen, R. Transposable elements and the epigenetic regulation of the genome. *Nat. Rev. Genet.* **8**, 272–285 (2007).
3. Brennecke, J. et al. Discrete small RNA-generating loci as master regulators of transposon activity in *Drosophila*. *Cell* **128**, 1089–1103 (2007).
4. Li, W. et al. Activation of transposable elements during aging and neuronal decline in *Drosophila*. *Nat. Neurosci.* **16**, 529–531 (2013).
5. Wood, J. G. et al. Chromatin-modifying genetic interventions suppress age-associated transposable element activation and extend life span in *Drosophila*. *Proc. Natl. Acad. Sci. USA* **113**, 11277–11282 (2016).
6. Burns, K. H. Transposable elements in cancer. *Nat. Rev. Cancer* **17**, 415–424 (2017).
7. Li, W., Jin, Y., Prazak, L., Hammell, M. & Dubnau, J. Transposable elements in TDP-43-mediated neurodegenerative disorders. *PLoS One* **7**, e44099 (2012).

8. Li, W. et al. Human endogenous retrovirus-K contributes to motor neuron disease. *Sci. Transl. Med.* **7**, 307ra153 (2015).
9. Krug, L. et al. Retrotransposon activation contributes to neurodegeneration in a *Drosophila* TDP-43 model of ALS. *PLoS Genet.* **13**, e1006635 (2017).
10. Frost, B., Hemberg, M., Lewis, J. & Feany, M. B. Tau promotes neurodegeneration through global chromatin relaxation. *Nat. Neurosci.* **17**, 357–366 (2014).
11. Wittmann, C. W. et al. Tauopathy in *Drosophila*: neurodegeneration without neurofibrillary tangles. *Science* **293**, 711–714 (2001).
12. Hutton, M. et al. Association of missense and 5′-splice-site mutations in tau with the inherited dementia FTDP-17. *Nature* **393**, 702–705 (1998).
13. Steinhilb, M. L., Dias-Santagata, D., Fulga, T. A., Felch, D. L. & Feany, M. B. Tau phosphorylation sites work in concert to promote neurotoxicity in vivo. *Mol. Biol. Cell* **18**, 5060–5068 (2007).
14. Dias-Santagata, D., Fulga, T. A., Duttaroy, A. & Feany, M. B. Oxidative stress mediates tau-induced neurodegeneration in *Drosophila*. J. *Clin. Invest.* **117**, 236–245 (2007).
15. Khurana, V. et al. A neuroprotective role for the DNA damage checkpoint in tauopathy. *Aging Cell* **11**, 360–362 (2012).
16. Frost, B., Bardai, F. H. & Feany, M. B. Lamin dysfunction mediates neurodegeneration in tauopathies. *Curr. Biol.* **26**, 129–136 (2016).
17. Merlo, P. et al. p53 prevents neurodegeneration by regulating synaptic genes. *Proc. Natl. Acad. Sci. USA* **111**, 18055–18060 (2014).
18. Khurana, V. et al. TOR-mediated cell-cycle activation causes neurodegeneration in a *Drosophila* tauopathy model. *Curr. Biol.* **16**, 230–241 (2006).
19. Geiss, G. K. et al. Direct multiplexed measurement of gene expression with color-coded probe pairs. *Nat. Biotechnol.* **26**, 317–325 (2008).
20. Bardai, F. H. et al. A conserved cytoskeletal signaling cascade mediates neurotoxicity of FTDP-17 tau mutations in vivo. *J. Neurosci.* **38**, 108–119 (2018).
21. Reilly, M. T., Faulkner, G. J., Dubnau, J., Ponomarev, I. & Gage, F. H. The role of transposable elements in health and diseases of the central nervous system. *J. Neurosci.* **33**, 17577–17586 (2013).
22. Muotri, A. R. et al. Somatic mosaicism in neuronal precursor cells mediated by L1 retrotransposition. *Nature* **435**, 903–910 (2005).
23. Pélisson, A. et al. About the origin of retroviruses and the co-evolution of the gypsy retrovirus with the *Drosophila* flamenco host gene. *Genetica* **100**, 29–37 (1997).
24. Mével-Ninio, M., Pelisson, A., Kinder, J., Campos, A. R. & Bucheton, A. The flamenco locus controls the gypsy and ZAM retroviruses and is required for *Drosophila* oogenesis. *Genetics* **175**, 1615–1624 (2007).
25. Frost, B., Götz, J. & Feany, M. B. Connecting the dots between tau dysfunction and neurodegeneration. *Trends Cell Biol.* **25**, 46–53 (2015).
26. Sarot, E., Payen-Groschêne, G., Bucheton, A. & Pélisson, A. Evidence for a piwi-dependent RNA silencing of the gypsy endogenous retrovirus by the *Drosophila melanogaster* flamenco gene. *Genetics* **166**, 1313–1321 (2004).
27. Roy, J., Sarkar, A., Parida, S., Ghosh, Z. & Mallick, B. Small RNA sequencing revealed dysregulated piRNAs in Alzheimer's disease and their probable role in pathogenesis. *Mol. Biosyst.* **13**, 565–576 (2017).
28. Qiu, W. et al. Transcriptome-wide piRNA profiling in human brains of Alzheimer's disease. *Neurobiol. Aging* **57**, 170–177 (2017).
29. Siomi, M. C., Sato, K., Pezic, D. & Aravin, A. A. PIWI-interacting small RNAs: the vanguard of genome defence. *Nat. Rev. Mol. Cell Biol.* **12**, 246–258 (2011).
30. Ghildiyal, M. et al. Endogenous siRNAs derived from transposons and mRNAs in *Drosophila* somatic cells. *Science* **320**, 1077–1081 (2008).
31. Lee, E. J. et al. Identification of piRNAs in the central nervous system. *RNA* **17**, 1090–1099 (2011).
32. Zamparini, A. L. et al. Vreteno, a gonad-specific protein, is essential for germline development and primary piRNA biogenesis in *Drosophila*. *Development* **138**, 4039–4050 (2011).
33. Eissenberg, J. C., Morris, G. D., Reuter, G. & Hartnett, T. The heterochromatin-associated protein HP-1 is an essential protein in *Drosophila* with dosage-dependent effects on position-effect variegation. *Genetics* **131**, 345–352 (1992).
34. Reuter, G., Dorn, R., Wustmann, G., Friede, B. & Rauh, G. Third chromosome suppressor of position-effect variegation loci in *Drosophila melanogaster*. *Mol. Gen. Genet.* **202**, 481–487 (1986).
35. Fedoroff, N. V. Presidential address. Transposable elements, epigenetics, and genome evolution. *Science* **338**, 758–767 (2012).
36. Longo, V. D. et al. Interventions to slow aging in humans: are we ready? *Aging Cell* **14**, 497–510 (2015).
37. Sultana, T., Zamborlini, A., Cristofari, G. & Lesage, P. Integration site selection by retroviruses and transposable elements in eukaryotes. *Nat. Rev. Genet.* **18**, 292–308 (2017).
38. Coates, J. A. et al. (−)-2′-Deoxy-3′-thiacytidine is a potent, highly selective inhibitor of human immunodeficiency virus type 1 and type 2 replication in vitro. *Antimicrob. Agents Chemother.* **36**, 733–739 (1992).
39. Andersen, P. R., Tirian, L., Vunjak, M. & Brennecke, J. A heterochromatin-dependent transcription machinery drives piRNA expression. *Nature* **549**, 54–59 (2017).
40. Brower-Toland, B. et al. *Drosophila* PIWI associates with chromatin and interacts directly with HP1a. *Genes Dev.* **21**, 2300–2311 (2007).
41. Klattenhoff, C. et al. The *Drosophila* HP1 homolog Rhino is required for transposon silencing and piRNA production by dual-strand clusters. *Cell* **138**, 1137–1149 (2009).
42. Gonzalez-Cao, M. et al. Human endogenous retroviruses and cancer. *Cancer Biol. Med.* **13**, 483–488 (2016).
43. Tyagi, R., Li, W., Parades, D., Bianchet, M. A. & Nath, A. Inhibition of human endogenous retrovirus-K by antiretroviral drugs. *Retrovirology* **14**, 21 (2017).
44. Chuong, E. B., Elde, N. C. & Feschotte, C. Regulatory evolution of innate immunity through co-option of endogenous retroviruses. *Science* **351**, 1083–1087 (2016).
45. Heneka, M. T., Golenbock, D. T. & Latz, E. Innate immunity in Alzheimer's disease. *Nat. Immunol.* **16**, 229–236 (2015).

Acknowledgements

We thank J. Dubnau (Stony Brook University) for gypsy-TRAP, R. Lehmann (New York University School of Medicine) for piwiOE, and M. Feany for tau^{R406W} and tau^{WT} *Drosophila* stocks. We acknowledge the Texas Advanced Computing Center (TACC; http://www.tacc.utexas.edu) at the University of Texas at Austin for providing high-performance computing resources. This study was supported by the National Institute for Neurological Disorders and Stroke (B.F.) and the Owens Foundation (B.F.). The Mayo human RNA-seq study data was led by N. Ertekin-Taner (Mayo Clinic) as part of the multi-PI U01 AG046139 (MPIs Golde, Ertekin-Taner, Younkin, Price) using samples from the Mayo Clinic Brain Bank. Data collection was supported through funding by NIA grants P50 AG016574, R01 AG032990, U01 AG046139, R01 AG018023, U01 AG006576, U01 AG006786, R01 AG025711, R01 AG017216 and R01 AG003949, NINDS grant R01 NS080820 and the CurePSP Foundation, and support from the Mayo Foundation.

Author contributions

W.S. and B.F. conceived the study and analyzed the data. W.S. and M.G. performed experiments. H.S. and H.Z. performed RNA-seq analysis. W.S., H.Z. and B.F. contributed to writing the manuscript. All authors reviewed the manuscript.

Competing interests

The authors declare no competing interests.

Additional information

Supplementary information is available for this paper at https://doi.org/10.1038/s41593-018-0194-1.

Reprints and permissions information is available at www.nature.com/reprints.

Correspondence and requests for materials should be addressed to B.F.

Publisher's note: Springer Nature remains neutral with regard to jurisdictional claims in published maps and institutional affiliations.

Methods

***Drosophila* genetics.** *Drosophila* crosses and aging were performed at 25 °C with a 12 h light/dark cycle at 60% relative humidity on a standard diet (Bloomington formulation). Full genotypes are listed in Supplementary Table 1. Pan-neuronal expression of transgenes, including RNAi-mediated knockdown, in *Drosophila* was achieved using the GAL4/UAS system[46] with the *elav* promoter driving GAL4 expression. Retinal expression of transgenes in gypsy-TRAP studies was achieved using the retinal *glass multiple reporter* (*GMR*) promoter. *elav-GAL4/+*, *GMR-Tau*^{V337M}, *UAS-GFP*, *flam*^{KG00476}, *flam*^{OR}, *Su(var)205*[5] and *Su(var)3-9*^{2} were obtained from the Bloomington Stock Center. *piwi*^{v101658} and *piwi*^{v22235} were obtained from the Vienna *Drosophila* Resource Center[47] (VDRC, http://www.vdrc.at). *UAS-tau*^{R406W} and *UAS-tau*^{WT} were a gift from Mel Feany. Gypsy-TRAP was a gift from Josh Dubnau. *UAS-HA-piwi* was a gift from Ruth Lehmann. An equal number of males and females were used in all *Drosophila* assays with the exception of gypsy-TRAP and *flamenco* genetic manipulations. Experiments using the gypsy-TRAP reporter or *flamenco* require two genetic elements on the X chromosome, and thus all data points are from female flies.

RNA sequencing and data analyses. Library preparation and sequencing were performed by the Genome Sequencing Facility at Greehey Children's Cancer Research Institute at the University of Texas Health San Antonio. For standard RNA-seq, three independent biologically independent replicates were sequenced, each consisting of 500 ng of total RNA from 6 pooled *Drosophila* heads (18 heads total). Extracted RNA was used for library preparation according to the KAPA Stranded RNA-seq Kit with RiboErase (HMR) sample preparation guide. After quantification by Qubit and Bioanalysis, libraries were pooled for cBot amplification and sequenced on the Illumina HiSeq 3000 platform with 100-base-pair paired-end sequencing.

For small RNA-seq, four independent biological replicates were sequenced. 500 ng of total RNA from pooled *Drosophila* heads was used for library preparation according to the NEBNext small RNA sample preparation guide. Due to the abundance of the 2 S rRNA in *Drosophila*, we included an additional 2 S blocking step using the oligonucleotide 5′-TAC AAC CCT CAA CCA TAT GTA GTC CAA GCA/3SpC3/-3′ as described[48]. 2 S rRNA blocking was performed directly after 3′ SR adaptor ligation. 1 µM of the 2 S rRNA blocking oligonucleotide was added directly to each ligation reaction on ice, and reactions were incubated at 90 °C for 30 s, then 65 °C for 5 min. After 5 min, we added 1 µl of SR RT primer and proceeded as described in the NEBNext protocol. After small RNA-seq libraries were quantified by Qubit and Bioanalysis, samples were pooled for cBot amplification and sequenced on the Illumina HiSeq 3000 platform with 50-base-pair single-read sequencing. After standard and small-RNA sequencing, CASAVA was used for demultiplexing and fastq files were generated for each sample.

For data cleaning, SortMeRNA[49] v2.1 was used to identify and exclude ribosomal RNA reads, and Trimmomatic[50] v0.36 was used to remove Illumina adaptors. FastQC (http://www.bioinformatics.babraham.ac.uk/projects/fastqc/) v0.11.5 was used for a quality check before and after the above cleaning steps. The quality of bases in the cleaned reads was above 28 (Sanger/Illumina 1.9 encoding). Reads were aligned to the transposon reference FASTA files (FlyBase[51] release 6.12), and the quantity of each transposable element was calculated using Salmon[52] v0.7.2. On average, 9 million reads were mapped per sample. DESeq2[53] v1.14.1 was used to identify sequences that were differentially expressed in tau transgenic *Drosophila* compared to controls. Ensembl BioMarts[54] was used to assign genomic locations of differentially expressed transcripts (Supplementary Table 2). Pheatmap (https://CRAN.R-project.org/package=pheatmap) v1.0.8 and Pigengene[55] v1.3.4 R[56] packages were used to generate heat maps. Values in transposable element heat maps are standardized transcripts per million[57] (TPM). For presentation clarity in Fig. 1, we subtracted the TPM value of each transposable element from its average across all samples and then divided the difference by the s.d. of the TPM value of that particular transposable element. Unscaled heat maps (Supplementary Fig. 1) represent raw TPM.

piRNA small RNA-seq analyses were similar to the above, with some exceptions. As some tRNAs are misannotated as piRNAs, piRNAs that were a subsequence of a tRNA (FlyBase[51] release 6.16) were removed from analysis. Reads were mapped to the remaining piRNA sequences (piRNABank[58]) as the reference. On average, 16 million reads were mapped per sample. piRNAs with low coverage were excluded as follows. If the sum of reads that mapped to a piRNA in all four tau transgenic *Drosophila* samples was less than 3, we considered its expression undetectable in tau transgenic samples. Similarly, if the sum of reads that mapped to a piRNA in all four control normal samples was less than 3, we considered its expression undetectable in controls. If a piRNA had undetectable expression values both tau transgenic and control samples, it was excluded from our analysis. Raw data for small RNA-seq are included in Supplementary Table 5, and genomic locations of differentially expressed piRNAs are included in Supplementary Table 6.

NanoString. We worked with bioinformaticians at NanoString Technologies, Inc. to create a custom codeset consisting of 50 probes: 47 transposable elements identified as differentially expressed by RNA-seq, plus three internal control genes (*RpL32*, *CG15117*, *cyp33*). Codeset sequences are included in Supplementary Table 3. 100 ng of total RNA from pooled *Drosophila* heads was used for NanoString nCounter XT Codeset Gene Expression Assays according to the manufacturer's protocol. Samples were analyzed by the nCounter Prep Station, and results were analyzed using the nCounter Digital Analyzer.

Immunofluorescence and histology. For tau, piwi and GFP immunofluorescence, *Drosophila* brains were dissected in PBS and fixed in methanol for 20 min. After blocking with 2% milk in 0.3% Triton in PBS for 30 min, brains were incubated with primary antibody diluted in blocking solution overnight at 4 °C. After washing with 0.3% Triton in PBS, brains were incubated with Alexa488- or Alexa555-conjugated secondary antibodies for 2 h at room temperature. Slides were washed again and incubated with DAPI for 2 min to stain nuclei. Brains were visualized by confocal microscopy (Zeiss LSM 780 NLO with Examiner), and ImageJ was used for analysis. All images shown are a single slice. TUNEL staining was performed in 4-µm sections from formalin-fixed, paraffin-embedded *Drosophila* heads. Secondary detection was performed with DAB. TUNEL-positive neurons were counted throughout the entire brain by bright field microscopy. Antibody concentrations and sources are listed in Supplementary Table 8.

Western blotting. Frozen *Drosophila* heads were homogenized in 20 µl Laemmli sample buffer, boiled for 10 min, and analyzed by 4–20% SDS–PAGE. After transfer to nitrocellulose membranes, antigen retrieval was performed by microwaving membranes in 1 L of PBS for 15 min. Equal loading was assessed by Ponceau S staining. After blocking membranes in PBS plus 0.05% Tween and 2% milk, membranes were incubated with primary antibodies overnight at 4 °C. After washing, membranes were incubated with HRP-conjugated secondary antibodies for 2 h at room temperature. Blots were developed with an enhanced chemiluminescent substrate. Antibody concentrations and sources are listed in Supplementary Table 8. Full scans of western blots are provided in Supplementary Fig. 10.

Locomotor activity. Walking activity was assayed as described previously[10].

Dietary restriction and 3TC treatment. 'Standard' diet consists of 1.5% yeast, 6.6% light corn syrup, 0.9% soy flour, 6.7% yellow cornmeal, 0.5% agar. 'Dietary restriction' diet consists of 0.5% yeast, 2.2% light corn syrup, 0.9% soy flour, 6.7% yellow cornmeal, 0.5% agar (all wt/vol). Flies were collected at day 1 of adulthood and placed on a standard or restricted diet. Flies were transferred to fresh food every other day until they were 10 d old, at which point they were fixed, frozen or assessed for locomotor activity.

For drug treatment, flies were collected at 2 d old and transferred to standard food or food containing 3TC (Fisher, no. 50731692, 10 mM except in Supplementary Fig. 3), which was dissolved in water. Flies were transferred to fresh food every other day until they were 10 d old, at which point they were fixed, frozen or assessed for locomotor activity.

Analysis of human RNA-seq data. The Mayo RNA-seq Study on Neuropathological Diseases generated whole-transcriptome data for cerebellum and temporal cortex samples from 312 North American subjects of European ancestry. These subjects were diagnosed with Alzheimer's disease, progressive supranuclear palsy or pathologic aging, or were elderly controls without neurodegenerative disorders[59]. We downloaded the corresponding clinical data (covariates) from the Accelerating Medicines Partnership – Alzheimer's Disease (AMP-AD) Knowledge Portal[60]. Specifically, we used the synapseClient R package v1.15-0 (http://docs.synapse.org/articles/getting_started.html) to download temporal cortex (syn5223705) and cerebellum (syn3817650) clinical data. Twelve cortex (syn6126114) and 10 cerebellum (syn6126119) samples were excluded due to low quality[61,62]. In this study, we also excluded 9 cortex and 15 cerebellum samples that had an RNA integrity number (RIN)[63] less than 7. After this filtering, 80 Alzheimer's disease, 82 progressive supranuclear palsy and 21 control cortex samples were available, along with 76 Alzheimer's disease, 78 progressive supranuclear palsy and 25 control cerebellum samples. Nilufer Taner at the Mayo Clinic provided us with unprocessed RNA-seq data. We converted raw bam files to fastq files using the Picard SamToFastq v2.10.10 tool (http://broadinstitute.github.io/picard). We downloaded human transposable elements from the Genetic Information Research Institute (GIRI) RepBase[64] database in fasta format (http://www.girinst.org/repbase/update/browse.php?type=All&format=FASTA&autonomous=on&nonautonomous=on&simple=on&division=Homo+sapiens&letter=A). The file contains 1,073 unique sequences, including the 549 ancestral repeats that are shared among all mammals. Using the same pipeline that we described for the analysis of *Drosophila* RNA-seq data, we cleaned the fastq files, aligned them to the human transposable element sequences, and performed differential expression analysis.

Principal component analyses (PCA) of human RNA-seq data. We used DESeq2 package and a likelihood ratio test to identify 19 transposable elements that have variable expression in any of the three Alzheimer's disease, progressive supranuclear palsy or control conditions in cortex (Supplementary Table 7). We then oversampled the control samples to balance the number of samples in each condition by repeating each control sample four times. We performed PCA

using the 19 differentially expressed transposable elements and the 80 Alzheimer's disease, 82 progressive supranuclear palsy and 84 control samples. A scatter plot of the first two principal components showed that Alzheimer's disease and progressive supranuclear palsy samples cluster together (Fig. 7d). We considered the median of this cluster over all Alzheimer's disease and progressive supranuclear palsy samples as the center of the cluster and computed the distance of each sample to the cluster center. A Kolmogorov–Smirnov test showed that the control samples do not generally belong to this cluster (Fig. 7e, $P<3\times10^{-7}$). We used the ggplot2[65] R package v 2.2.1 to generate violin plots. We performed a similar analysis on cerebellum, which showed that 20 transposable elements have variable expression in Alzheimer's disease, progressive supranuclear palsy or control (Supplementary Fig. 4a–c and Supplementary Table 7). We repeated each control cerebellum sample three times, which provided 75 control samples for PCA. Like the cortex samples, the 76 Alzheimer's disease and 78 progressive supranuclear palsy samples cluster together in the scatter plot, and control samples do not generally belong to this cluster (Supplementary Fig. 4d, $P<2\times10^{-6}$). In particular, the majority of control samples are below the orange diagonal line.

Over-representation of specific transposable element classes in differential expression analyses. All four transposable elements that are downregulated in Alzheimer's disease cortex are non-LTR retrotransposons. This is significantly more than expected, since only 239 (22%) of the total 1,073 human transposable elements are non-LTR (hypergeometric test, $P=0.002$). Similarly, the non-LTR retrotransposon are over-represented among downregulated transposable elements in progressive supranuclear palsy cortex ($P=5\times10^{-7}$). We used the sumlog function from the metap package v0.8 to combine these two P-values by Fisher's method ($P=2\times10^{-8}$). We multiplied the resulting P-value by 2 to adjust for the two tests conducted, cortex and cerebellum. Similarly, we confirmed that the non-LTR retrotransposon are also over-represented in the decreased transposable elements in cerebellum (adjusted $P=0.01$). We used similar tests to show that endogenous retroviruses are over-represented in the upregulated transposable elements in cortex (adjusted $P=0.004$) and cerebellum (adjusted $P=0.0003$).

Statistical analyses. Every reported n is the number of biologically independent replicates. Except when noted otherwise, statistical analyses were performed using a one-way ANOVA with Tukey test when comparing among multiple genotypes and a two-tailed, unpaired Student's t-test when comparing two genotypes. Data distribution was assumed to be normal, but this was not formally tested. For RNA-seq analysis, a two-sided Wald test[66] was used to calculate false discovery rates (FDR-adjusted P-value). For NanoString analyses, we used nSolver Analysis Software v3.0. The central tendency presented is the mean in all cases except NanoString data (median), and error bars represent s.e.m. A P-value less than 0.05 was considered significant unless otherwise specified. Sample sizes are similar to or greater than those reported in previous publications[4,5,10]. Samples were randomized in all *Drosophila* studies. Investigators were blinded to genotype in all immunohistochemistry, immunofluorescence and locomotor activity assays. Full statistical analyses are provided in Supplementary Table 9. To improve transparency and increase reproducibility, detailed information on experimental design and reagents can be accessed in the Life Sciences Reporting Summary.

Reporting Summary. Further information on experimental design is available in the Nature Research Reporting Summary linked to this article.

Accession codes. Full access to fastq files that include *Drosophila* transposable element and piRNA is provided through the Gene Expression Omnibus (GEO) database (GSE115606).

Code availability. Custom code that was created for cleaning and analyzing sequencing data is available in Supplementary Software and can also be accessed at https://bitbucket.org/habilzare/alzheimer/.

Data availability. Raw counts from RNA sequencing are provided as Supplementary Tables 2, 5 and 7. The data that support the findings of this study are available from the corresponding author upon reasonable request.

References

46. Fischer, J. A., Giniger, E., Maniatis, T. & Ptashne, M. GAL4 activates transcription in *Drosophila*. *Nature* **332**, 853–856 (1988).
47. Dietzl, G. et al. A genome-wide transgenic RNAi library for conditional gene inactivation in *Drosophila*. *Nature* **448**, 151–156 (2007).
48. Wickersheim, M. L. & Blumenstiel, J. P. Terminator oligo blocking efficiently eliminates rRNA from *Drosophila* small RNA sequencing libraries. *Biotechniques* **55**, 269–272 (2013).
49. Kopylova, E., Noé, L. & Touzet, H. SortMeRNA: fast and accurate filtering of ribosomal RNAs in metatranscriptomic data. *Bioinformatics* **28**, 3211–3217 (2012).
50. Bolger, A. M., Lohse, M. & Usadel, B. Trimmomatic: a flexible trimmer for Illumina sequence data. *Bioinformatics* **30**, 2114–2120 (2014).
51. Gramates, L. S. et al. FlyBase at 25: looking to the future. *Nucleic Acids Res.* **45**(D1), D663–D671 (2017).
52. Patro, R., Duggal, G., Love, M. I., Irizarry, R. A. & Kingsford, C. Salmon provides fast and bias-aware quantification of transcript expression. *Nat. Methods* **14**, 417–419 (2017).
53. Love, M. I., Huber, W. & Anders, S. Moderated estimation of fold change and dispersion for RNA-seq data with DESeq2. *Genome Biol.* **15**, 550 (2014).
54. Kinsella, R. J. et al. Ensembl BioMarts: a hub for data retrieval across taxonomic space. *Database (Oxford)* **2011**, bar030 (2011).
55. Foroushani, A. et al. Large-scale gene network analysis reveals the significance of extracellular matrix pathway and homeobox genes in acute myeloid leukemia: an introduction to the Pigengene package and its applications. *BMC Med. Genomics* **10**, 16 (2017).
56. R Development Core Team. R: A language and environment for statistical computing. http://www.R-project.org/(2010).
57. Wagner, G. P., Kin, K. & Lynch, V. J. Measurement of mRNA abundance using RNA-seq data: RPKM measure is inconsistent among samples. *Theory Biosci.* **131**, 281–285 (2012).
58. Sai Lakshmi, S. & Agrawal, S. piRNABank: a web resource on classified and clustered Piwi-interacting RNAs. *Nucleic Acids Res.* **36**, D173–D177 (2008).
59. Allen, M. et al. Human whole genome genotype and transcriptome data for Alzheimer's and other neurodegenerative diseases. *Sci. Data* **3**, 160089 (2016).
60. Hodes, R. J. & Buckholtz, N. Accelerating Medicines Partnership: Alzheimer's Disease (AMP-AD) Knowledge Portal aids Alzheimer's drug discovery through open data sharing. *Expert Opin. Ther. Targets* **20**, 389–391 (2016).
61. Purcell, S. et al. PLINK: a tool set for whole-genome association and population-based linkage analyses. *Am. J. Hum. Genet.* **81**, 559–575 (2007).
62. Price, A. L. et al. Principal components analysis corrects for stratification in genome-wide association studies. *Nat. Genet.* **38**, 904–909 (2006).
63. Schroeder, A. et al. The RIN: an RNA integrity number for assigning integrity values to RNA measurements. *BMC Mol. Biol.* **7**, 3 (2006).
64. Bao, W., Kojima, K. K. & Kohany, O. Repbase Update, a database of repetitive elements in eukaryotic genomes. *Mob. DNA* **6**, 11 (2015).
65. Wickham, H. *ggplot2: Elegant Graphics for Data Analysis* 2nd edn, Springer International, Basel, Switzerland (2016).
66. Wald, A. Tests of statistical hypotheses concerning several parameters when the number of observations is large. *Trans. Am. Math. Soc.* **54**, 426–482 (1943).

nature research

Corresponding author(s): Dr. Bess Frost

Reporting Summary

Nature Research wishes to improve the reproducibility of the work that we publish. This form provides structure for consistency and transparency in reporting. For further information on Nature Research policies, see Authors & Referees and the Editorial Policy Checklist.

Statistical parameters

When statistical analyses are reported, confirm that the following items are present in the relevant location (e.g. figure legend, table legend, main text, or Methods section).

n/a	Confirmed	
☐	☒	The exact sample size (*n*) for each experimental group/condition, given as a discrete number and unit of measurement
☐	☒	An indication of whether measurements were taken from distinct samples or whether the same sample was measured repeatedly
☐	☒	The statistical test(s) used AND whether they are one- or two-sided *Only common tests should be described solely by name; describe more complex techniques in the Methods section.*
☐	☒	A description of all covariates tested
☐	☒	A description of any assumptions or corrections, such as tests of normality and adjustment for multiple comparisons
☐	☒	A full description of the statistics including central tendency (e.g. means) or other basic estimates (e.g. regression coefficient) AND variation (e.g. standard deviation) or associated estimates of uncertainty (e.g. confidence intervals)
☐	☒	For null hypothesis testing, the test statistic (e.g. *F*, *t*, *r*) with confidence intervals, effect sizes, degrees of freedom and *P* value noted *Give P values as exact values whenever suitable.*
☒	☐	For Bayesian analysis, information on the choice of priors and Markov chain Monte Carlo settings
☒	☐	For hierarchical and complex designs, identification of the appropriate level for tests and full reporting of outcomes
☐	☒	Estimates of effect sizes (e.g. Cohen's *d*, Pearson's *r*), indicating how they were calculated
☐	☒	Clearly defined error bars *State explicitly what error bars represent (e.g. SD, SE, CI)*

Our web collection on statistics for biologists may be useful.

Software and code

Policy information about availability of computer code

Data collection

Drosophila: For standard RNA-seq, three independent biologically independent replicates were sequenced, each consisting of 500 ng of total RNA from six pooled Drosophila heads (18 heads total). Extracted RNA was used for library preparation according to the KAPA Stranded RNA-seq Kit with RiboErase (HMR) sample preparation guide. After quantification by Qubit and Bioanalysis, libraries were pooled for cBot amplification and sequenced on the Illumina HiSeq 3000 platform with 100 base pair paired-end sequencing.
For small RNA-seq, four independent biological replicates were sequenced. 500 ng of total RNA from pooled Drosophila heads was used for library preparation according to the NEBNext small RNA sample preparation guide. Due to the abundance of the 2S rRNA in Drosophila, we included an additional 2S block step using the oligo (5'-TAC AAC CCT CAA CCA TAT GTA GTC CAA GCA/3SpC3/-3') as described48. 2S rRNA blocking was performed directly after 3' SR adapter ligation. 1 µM of the 2S rRNA block oligo was added directly to each ligation reaction on ice, and reactions were incubated at 90°C for 30 sec, then 65°C for 5 min. After 5 min, 1 µl of SR RT primer was added and we proceeded as described in the NEBNext protocol. After small RNA-seq libraries were subjected to quantification by Qubit and Bioanalysis, samples were pooled for cBot amplification and sequenced on the Illumina HiSeq 3000 platform with 50 base pair single-read sequencing.

Human: The Mayo RNA-seq Study on Neuropathological Diseases generated whole transcriptome data for cerebellum and temporal cortex samples from 312 North American Caucasian subjects. These subjects were diagnosed with Alzheimer's disease, progressive supranuclear palsy, pathologic aging or were elderly controls without neurodegenerative disorders59. We downloaded the corresponding clinical data (covariates) from the Accelerating Medicines Partnership – Alzheimer's Disease (AMP-AD) Knowledge Portal60. Specifically, we used the synapseClient R package v1.15-0 (hp://www.sagebase.org) to download temporal cortex (syn5223705) and cerebellum (syn3817650) clinical data. Dr. Nilufer Taner at the Mayo Clinic provided us with unprocessed RNA-seq data.

Data analysis

Drosophila: After standard and small-RNA sequencing, CASAVA was used for demultiplexing and fastq files were generated for each sample.
For data cleaning, SortMeRNA49 v2.1 was used to identify and exclude ribosomal RNA reads, and Trimmomatic50 v0.36 was used to remove Illumina adaptors. FastQC (http://www.bioinformatics.babraham.ac.uk/projects/fastqc/) v0.11.5 was used for a quality check before and after the above cleaning steps. The quality of bases in the cleaned reads was above 28 (Sanger/Illumina 1.9 encoding). Reads were aligned to the transposon reference FASTA files (FlyBase51 Release 6.12), and the quantity of each transposable element was calculated using Salmon52 v0.7.2. On average, 9 million reads were mapped per sample. DESeq253 v1.14.1 was used to identify sequences that were differentially expressed in tau transgenic Drosophila compared to controls. Ensembl BioMarts54 was used to assign genomic locations of differentially expressed transcripts (Supplementary Table 2). Pheatmap (https://CRAN.R-project.org/package=pheatmap) v1.0.8 and Pigengene55 v1.3.4 R56 packages were used to generate heatmaps. Values in transposable element heatmaps are standardized Transcripts Per Million57 (TPM). For presentation clarity in Fig. 1, we subtracted the TPM value of each transposable element from its average across all samples, and then divided the difference by the standard deviation of the TPM value of that particular transposable element. Unscaled heatmaps (Supplementary Fig. 1) represent raw TPM.
piRNA small RNA-seq analyses were similar to the above, with some exceptions. As some tRNAs are mis-annotated as piRNAs, piRNAs that were a subsequence of a tRNA (FlyBase51 Release 6.16) were removed from analysis. Reads were mapped to the remaining piRNA sequences (piRNABank58) as the reference. On average, 16 million reads were mapped per sample. piRNAs with low coverage were excluded as follows: If the sum of reads that mapped to a piRNA in all four tau transgenic Drosophila samples was less than three, we considered its expression “undetectable” in tau transgenic samples. Similarly, if the sum of reads that mapped to a piRNA in all four control normal samples was less than three, we considered its expression undetectable in controls. If a piRNA had undetectable expression values both tau transgenic and control samples, it was excluded from our analysis. Raw data for small RNA-seq are included in Supplementary Table 5, and genomic locations of differentially expressed piRNAs are included in Supplementary Table 6.

Human: We converted raw bam files to fastq files using the Picard SamToFastq v2.10.10 tool (http://broadinstitute.github.io/picard). We downloaded human transposable elements from the Genetic Information Research Institute (GIRI) RepBase64 database in fasta format (http://www.girinst.org/repbase/update/browse.php?type=All&format=FASTA&autonomous=on&nonautonomous=on&simple=on&division=Homo+sapiens&letter=A). The file contains 1073 unique sequences including the 549 ancestral repeats that are shared among all mammals. Using the same pipeline that we described for the analysis of Drosophila RNA-seq data, we cleaned the fastq files, aligned them to the human transposable element sequences, and performed differential expression analysis.

For manuscripts utilizing custom algorithms or software that are central to the research but not yet described in published literature, software must be made available to editors/reviewers upon request. We strongly encourage code deposition in a community repository (e.g. GitHub). See the Nature Research guidelines for submitting code & software for further information.

Data

Policy information about availability of data

All manuscripts must include a data availability statement. This statement should provide the following information, where applicable:

- Accession codes, unique identifiers, or web links for publicly available datasets
- A list of figures that have associated raw data
- A description of any restrictions on data availability

Raw counts from RNA sequencing are provided as Supplementary Tables. Full access to bam files that include Drosophila transposable element and piRNA reads will be made publicly available upon publication. Custom codes that were created for cleaning and analyzing sequencing data will be made available upon publication.

Field-specific reporting

Please select the best fit for your research. If you are not sure, read the appropriate sections before making your selection.

☒ Life sciences ☐ Behavioural & social sciences ☐ Ecological, evolutionary & environmental sciences

For a reference copy of the document with all sections, see nature.com/authors/policies/ReportingSummary-flat.pdf

Life sciences study design

All studies must disclose on these points even when the disclosure is negative.

Sample size

Sample size was based on power analysis for the original submission. Sample sizes for TUNEL and PCNA were increased for the final submission based on a reviewer request.

Data exclusions

Exclusion criteria were pre-established prior to data analysis.
For Drosophila piRNA small RNA-seq analyses, as some tRNAs are mis-annotated as piRNAs, piRNAs that were a subsequence of a tRNA (FlyBase51 Release 6.16) were removed from analysis. Reads were mapped to the remaining piRNA sequences (piRNABank58) as the reference. piRNAs with low coverage were excluded as follows: If the sum of reads that mapped to a piRNA in all four tau transgenic Drosophila samples was less than three, we considered its expression "undetectable" in tau transgenic samples. Similarly, if the sum of reads that mapped to a piRNA in all four control normal samples was less than three, we considered its expression undetectable in controls. If a piRNA had undetectable expression values both tau transgenic and control samples, it was excluded from our analysis.
For human RNA-seq data, 12 cortex (syn6126114) and 10 cerebellum (syn6126119) samples were excluded due to low quality by the Mayo Clinic61,62. In this study, we also excluded 9 cortex and 15 cerebellum samples that had an RNA Integrity Number (RIN)63 less than 7.

	After this filtering, 80 Alzheimer's disease, 82 progressive supranuclear palsy, and 21 control cortex samples were available, as well as 76 Alzheimer's disease, 78 progressive supranuclear palsy, and 25 control cerebellum samples.
Replication	All attempts at replication were reproducible. For representative images, quantification of replicates is provided. For many experiments, multiple investigators repeated the same experiment. The number of independent experiments is presented in the figure legends and Supplementary Table 9.
Randomization	The order of Drosophila genotypes used for dissection/fixation/head homogenization was randomized for each experiment. The order of genotypes deposited in NanoString cartriges was also randomized.
Blinding	Blinding was performed for immunofluorescence and immunohistochemistry (including TUNEL and PCNA counting).

Reporting for specific materials, systems and methods

Materials & experimental systems

n/a	Involved in the study
☒	☐ Unique biological materials
☐	☒ Antibodies
☒	☐ Eukaryotic cell lines
☒	☐ Palaeontology
☐	☒ Animals and other organisms
☐	☒ Human research participants

Methods

n/a	Involved in the study
☒	☐ ChIP-seq
☒	☐ Flow cytometry
☒	☐ MRI-based neuroimaging

Antibodies

Antibodies used	Presented in Supplementary Table 8 Actin (Dm), Abcam #ab8227, dillution1:50,000, Secondary rHRP, SouthernBiotech #3010-05, dillution1:20,000; GFP (Dm), UCDavis/NIH NeuroMab #75-131, dillution 1:1000, secondary mHRP, SouthernBiotech #1010-05, dillution 1:10,000; PCNA (Dm), Dako #M0879, dillution 1:200, secondary rBio, SouthernBiotech #4010-08, dillution 1:200; piwi (Dm), Abcam #5207, dillution for WB 1:500, for IF 1:50, secondary rHRP for WB, SouthernBiotech #3010-05, dillution 1:1000, secondary r555 for IF, Thermo Fisher #A21434, dillution 1:200; cTau (Dm), Dako #A0024, dillution 1:2000,000, secondary rHRP, SouthernBiotech #3010-05, dillution 1:20,000.
Validation	GFP validated by western blot using Drosophila lines with and without transgenic GFP (data not shown); PCNA validated previously by genetic manipulation of cell cycle machinery (Khurana, V. et al. TOR-mediated cell-cycle activation causes neurodegeneration in a Drosophila tauopathy model. Current biology : CB 16, 230-241, doi:10.1016/j.cub.2005.12.042 (2006).) piwi validated by western blot, piwi RNAi Drosophila lines (Supp. Fig. 4a); cTau (Dm), Dako #A0024 - validated by western blot, tau transgenic and non-transgenic Drosophila (Supp. Fig. 2a) Actin was not validated but is widely used

Animals and other organisms

Policy information about studies involving animals; ARRIVE guidelines recommended for reporting animal research

Laboratory animals	Drosophila melanogaster - equal numbers of males/females were used unless otherwise noted. Age is day 10 of adulthood unless otherwise noted.
Wild animals	No wild animals were used in this study.
Field-collected samples	No field-collected samples were used in this study.

Human research participants

Policy information about studies involving human research participants

Population characteristics	*Describe the covariate-relevant population characteristics of the human research participants (e.g. age, gender, genotypic information, past and current diagnosis and treatment categories). If you filled out the behavioural & social sciences study design questions and have nothing to add here, write "See above."*
Recruitment	*Describe how participants were recruited. Outline any potential self-selection bias or other biases that may be present and how these are likely to impact results.*